Journal of
Advanced Civil and Environmental Engineering
Vol.6, No.2, 2023, pp 107-117
ISSN: 2599-3356
DOI: http://dx.doi.org/10.30659/jacee.6.2.107-117

Numerical Analysis of Soft Soil Improvement using Pile at Airport Construction Project

Himatul Farichah[1*], Dio Alif Hutama[2], and Dian Purnamawati Solin[1]

[1]*Civil Engineering Department, Engineering Faculty, Universitas Pembangunan Nasional Veteran Jawa Timur, Rungkut Madya No 1 Surabaya, 60294, Indonesia*
[2]*Study Program of Environmental Engineering, Department of Biology, Faculty of Science and Technology, Universitas Airlangga, Kampus C UNAIR, Jalan Dr. Ir. H. Soekarno, Surabaya 60115, Indonesia*

* *Corresponding author: himatul_farichah.ts@upnjatim.ac.id*

(**Received:** 6th February 2023 ; **Revised:** 20th November 2023 ; **Accepted:** 20th November 2023)

Abstract: Construction on the soft ground poses an excellent challenge for geotechnical engineers. Several engineering problems such as bearing capacity failure and differential settlement could occur either during or after the construction phase due to high compressibility and low shear strength. Nowadays, a number of soil improvement techniques are available to solve such problems. However, each method has its advantages and disadvantages. In this study, soil improvement analysis using pile were performed with three variations depths so called 12 m, 18 m, and 24 m from the ground level. A finite element simulation has been performed using PLAXIS 2D. The pile has been modeled as plate and Mohr-Coulomb model was used for soil model. The results show that the deeper the pile, the settlement will be decreasing. Moreover, the axial force and bending moment of the pile obtained from the output of PLAXIS 2D were also presented to assess the performance of the soil improvement technique.

Keywords: Soft Soil, Soil Improvement, Pile

1. Introduction

Construction buildings on soft ground areas is a major challenge in the geotechnical engineering field. Engineering problems could be found in the construction on soft soil due to its low bearing capacity and high compressibility of soft soil [1]. To minimize the issues that might occur in the construction of soft soil, soil improvement methods are mainly required. There are several soil improvement methods commonly applied in Indonesia, such as soil preloading with a combination of PVD (Prefabricated vertical drain) [2] or vacuum [3] [4], compaction [5][6], soil reinforcement [7], pile [8], etc. Each soil improvement technique has advantages and disadvantages.

The improvement method using piles is expected that piles with greater strength and stiffness than the surrounding soil can carry most of the load from the upper structure. Thus, the settlement can be reduced without soil excavation or replacement. In principle, piles can be categorized into 3 (three) categories, namely flexible piles (such as sand piles, stone columns, and lime columns), semi-rigid piles (such as soil-cement columns), and rigid piles (such as concrete piles) [9]. The term "pile" in this study is a rigid pile (concrete pile). Several studies have demonstrated the use of piles as an improvement method for soft soils [10], [11].

A case study in this article is the airport developments, especially for apron expansion. At that location, the soil condition was found to be dominated by clay with N-SPT below 10 to a depth of almost 15 m. Therefore, this study presents a numerical analysis of soil improvement was carried out using piles with the PLAXIS 2D program. In this study, the effect of the length of the pile on the maximum settlement of the soil surface and the moment and axial forces that occur on the pile is studied. In this study, three variation depths of the piles are used; they are 12 m, 18 m, and 24 m.

2. Research Method

This study takes a case study in one of the airport expansion projects in Indonesia with 2 (two) work packages, namely apron expansion and taxiway expansion. In this study, only apron expansion will be discussed and analyzed with the soil condision shown in Fig. 1.

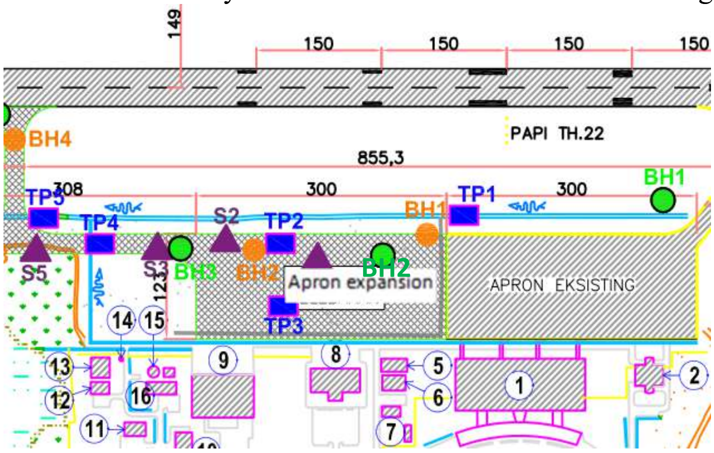

Fig. 1. Layout of airport project

In Fig. 1, there is sondir data symbolized by the letter S and a purple triangular shape. Then for SPT-N soil data is represented by BH and the shape of orange and green circles. The orange color shows the latest soil data, which this study considers. At the location of the apron expansion, 2 (two) SPT-N soil data were taken, namely BH-01 and BH-02. SPT-N value versus the depth was then plotted as shown in Fig 2. From Fig. 2, it can be seen that BH-02 has a lower NSPT value, so BH-02 is used in soil improvement analysis. Soil conditions in BH-02 are as follows; sandy soil at a depth of 0-2 m, clay at a depth of 2-4 m, clayey sand at a depth of 4-10 m, clay at a depth of 10-16 m, and stiff clay at a depth of 16-30 m. In general, the soil type at this location is dominated by clay, with an elevation of the groundwater level found at the ground surface (GWL=0 meter).

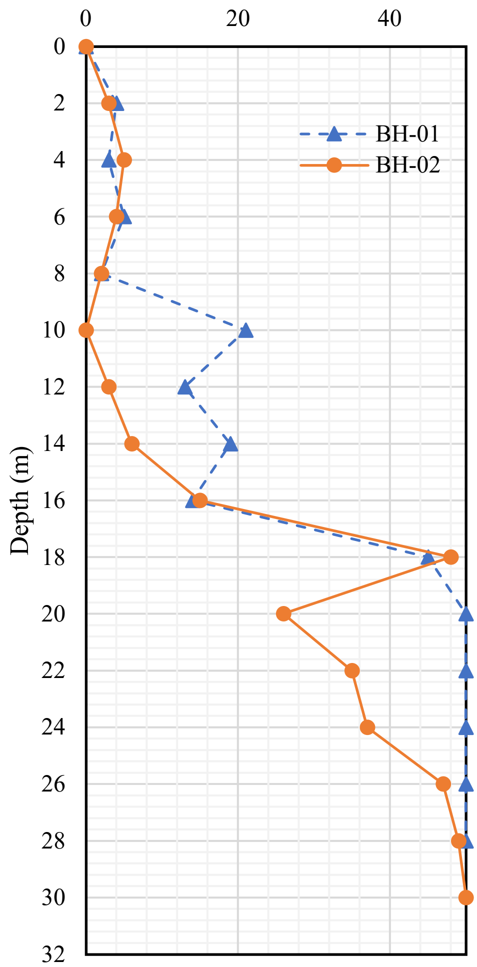

Fig. 2. SPT-N Value

Table 1. Correlation of SPT-N value [12]

	Cohesionless soil				
N	0-3	4-10	11-30	31-50	>50
(γ)kN/m³	-	12-16	14-18	16-20	18-23
(φ)	-	25-32	28-36	30-40	>35
State	Very loose	Loose	medium	dense	Very dense
	Cohesive soil				
N	< 4	4-6	6-15	16-25	>25
(γ) kN/m³	14-18	16-18	16-18	16-18	>20
(qu)	< 25	20-50	30-60	40-200	>100
Consistency	Very soft	soft	medium	Stiff	Hard

Soil stratigraphy was then generated according to the SPT-N values and soil consistency. For the input of soil parameters in PLAXIS, analysis and interpretation of bor-log and NSPT data are carried out. Empirical correlations were carried out using Table 1 to Table 5 to obtain all input parameters in PLAXIS. SPT-N values and the results of boring investigations that provide soil type information are correlated to get soil consistency, unit weight (γ), saturated unit weight (γ_{sat}), cohesion (Cu), friction angle (φ), elastic modulus (E), permeability (k), and the Poisson ratio (υ).

Table 2. Typical values of permeability for various soil types [13]

Soil Type	K (cm/s)
Clean gravel	100-1
Coarse sand	1-0.01
Fine sand	0.01-0.001
Silty clay	0.001-0.00001
Clay	<0.0000001

Table 3. Typical values of elastic modulus for various soil types [14]

Soil Type		**E_s (kN/m^2)**
Clay	Very Soft	2000-15000
	Soft	2000-25000
	Medium	15000-50000
	Hard	50000-100000
	Sandy	25000-250000
Glacial till	Loose	10000-153000
	Dense	144000-720000
	Very dense	478000-1440000
	Loess	15000-60000
Sand	Silty	5000-20000
	Loose	10000-25000
	Dense	50000-81000
Sand and Gravel	Loose	50000-150000
	Dense	100000-200000
Shale		150000-5000000
Silt		2000-20000

Table 4. Typical Values of Poisson's ratio [14]

Material	Possion's Rasio (v)
Clay, Saturated	0.40-0.50
Clay, unsaturated	0.10-0.30
Sandy clay	0.20-0.30
Silt	0.30-0.35
Gravelly Sand	0.10-1.00
Sand	0.30-0.40
Rock	0.10-0.40
Loess	0.10-0.30

The load entered into PLAXIS is the design load for apron planning. The design load for planning the apron is the maximum aircraft load, the Boeing 737-900 ER, is loaded to a uniform load of 10 kPa (assumed). Loading details can be seen in Table 5.

Tabel 5. Total equivalent load

Material	Thikness (m)	Unit Weight (kN/m^3)	q (kN/m^2)
Concrete slab	0.45	24	10.8
Lean concrete	0.15	23.6	3.54
Base course	0.2	14.5	2.9
Sub-base course	0.15	15.4	2.31
Aircraft load			10
Sand	0.5	18	9
		Total Equivalent Load	**38.55**

The type of pile used are prestressed concrete square piles with the size of 200x200 mm class A and have a bending moment crack of 1.55 (ton.m) and allowable compression of 49.08 (tons). The piles are designed with a spacing of 1.5 m and 3 (three) variations of depth, namely 12 m, 18 m, and 24 m. The piles are modeled using the plate and plane strain approach in PLAXIS.

The conversion process for circular piles is changed to a square shape and then to a plane stain. In this conversion, I (inertia) and E are influential values. The transformation from circle-shape properties to plane strain properties is discussed.

I, A (area), and E for circle properties:

$$A_{circle} = \frac{1}{4}\pi d^2 \quad (1)$$

$$I_{circle} = \frac{1}{64}\pi d^4 \quad (2)$$

Convert to square properties:

$$S_{square} = \sqrt{A_{circle}} \quad (3)$$

$$I_{square} = \frac{1}{12} S_{square}{}^4 \quad (4)$$

$$E_{square} = \frac{E_{circle} \times I_{circle}}{I_{square}} \quad (5)$$

Convert to plane strain properties:

$$h = S_{square}, b = 1 \quad (6)$$

$$A_{plane\ strain} = b \times h \quad (7)$$

$$I_{plane\ strain} = \frac{1}{12} b \times h^3 \quad (8)$$

$$E_{plane\ strain} = \frac{E_{square} \times I_{square}}{I_{plane\ strain}} \quad (9)$$

$$Axial\ stiffness = \frac{E \times A}{spacing} \quad (10)$$

$$Bending\ stiffness = \frac{E \times I}{spacing} \quad (11)$$

$$W = A \times \gamma_{concrete} \quad (12)$$

Then from the running results, the SF value, failure pattern, deformation and internal force on the pile can be seen. Then proceed in the same way with variations in pile depth. The results of running and analysis for depth variations will be used to formulate conclusions and suggestions for this study.

3. Results and Discussion

Analysis of the bearing capacity of subgrade soil was carried out based on the bearing capacity formula of Terzaghi (Terzaghi, 1943) with soil data from the results of BH-02 soil investigation as follows:

SPT-N Average (Navg)	= 3
Cu (Undrained Cohesion)	= 18 kPa
Nc (Bearing capacity factor)	= 5.14
Ultimit bearing capasity (Qult)	= 92.5 kPa
Allowable bearing capacity (Qall)	= 30.8 kPa
Safety factor (SF)	= Qall/total equivalent load= 30.8/38.55= 0.8 (SF < 1)

From the calculation results, the bearing capacity does not meet the design criteria (SF<1), so it is necessary to improve the soil so that failure does not occur during operation. An alternative used as a soil improvement method is using piles. The pile parameters inputted to PLAXIS are shown in Table 6.

Table 6. Parameters of pile stiffness

Stiffness parameters	Value
EA	613.300 kN/m
EI	2044 kN/m^2/m
W	0.2 kN/m/m

At PLAXIS, there are two stages of construction. The first is the installation of piles; the next is the provision of a distributed equivalent load of 38.55 kN/m^2 modeled as an evenly distributed load A in PLAXIS (Fig. 3-Fig. 5) as with variations in pile depth.

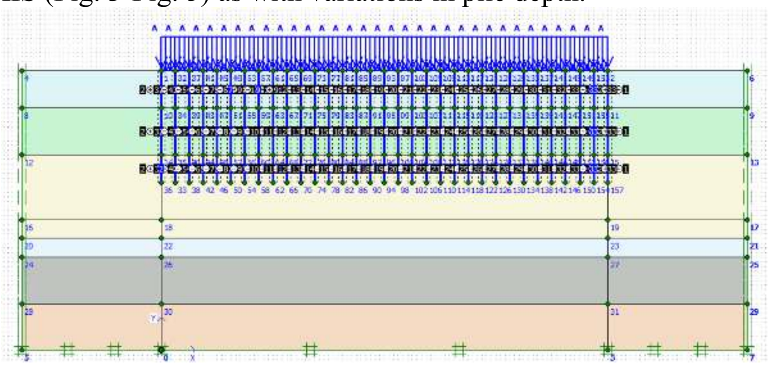

Fig. 3. Modeling at PLAXIS for a pile depth of 12 m

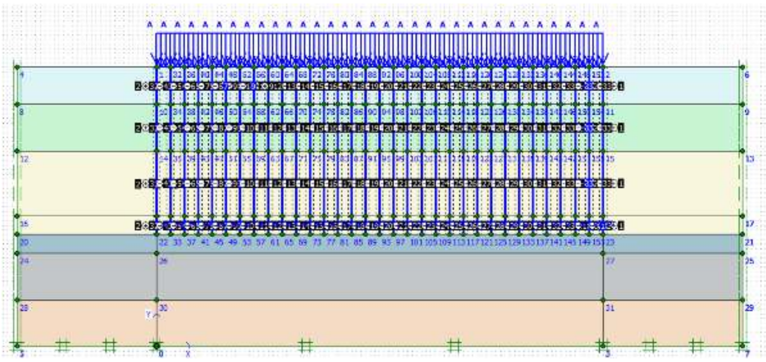

Fig. 4. Modeling at PLAXIS for a pile depth of 18 m

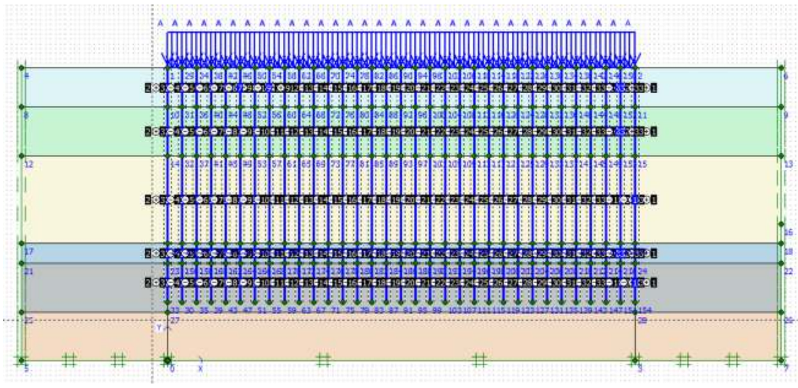

Fig. 5. Modeling at PLAXIS for a pile depth of 24 m

The modeling results from PLAXIS also found that vertical deformation occurs in the subgrade when loaded with a load equivalent to the three variations in pile depth, as shown in Fig. 6 to Fig. 8.

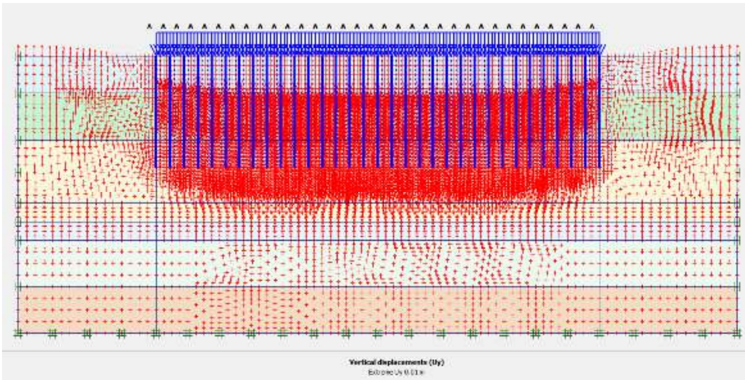

Fig. 6. Vertical deformation for variations in pile depth of 12 m

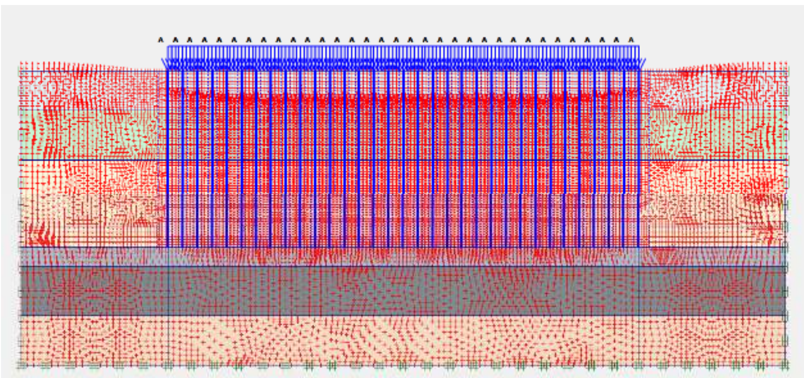

Fig. 7. Vertical deformation for variations in pile depth of 18 m

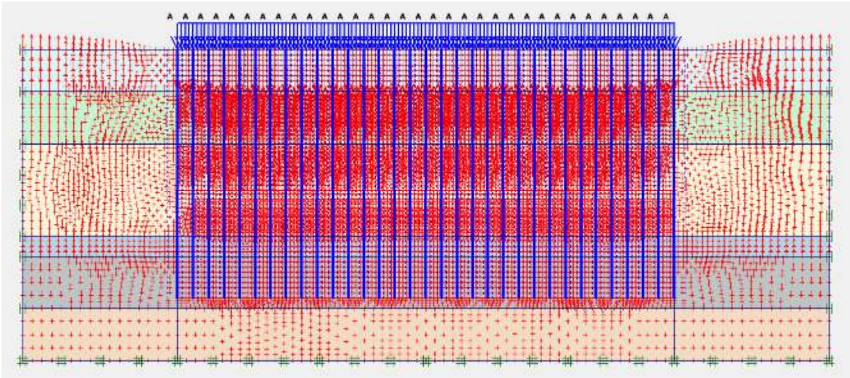

Fig. 8. Vertical deformation for variations in pile depth of 24 m

Apart from vertical deformation, from the output of PLAXIS, the internal forces that occur in a pile are also obtained. The axial force (kN) and bending moment (kN.m) are shown in Fig. 9 to Fig. 14. A summary of the largest settlement/settlement, bending moment, and axial force experienced by the pile for each depth variation can be seen in Table 7.

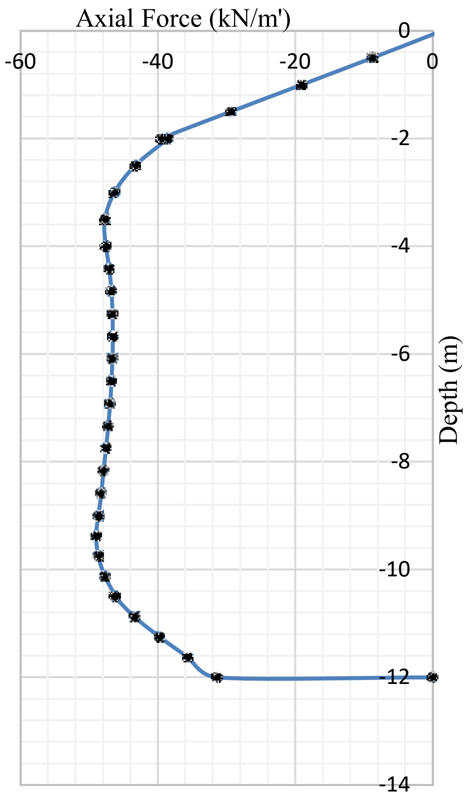

Fig. 9. The largest axial of pile for variations in pile depth of 12 m

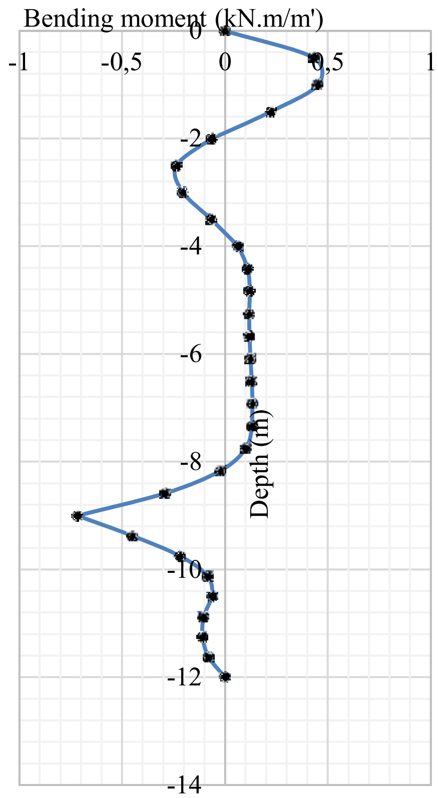

Fig. 10. The largest bending moment of pile for variations in pile depth of 12 m

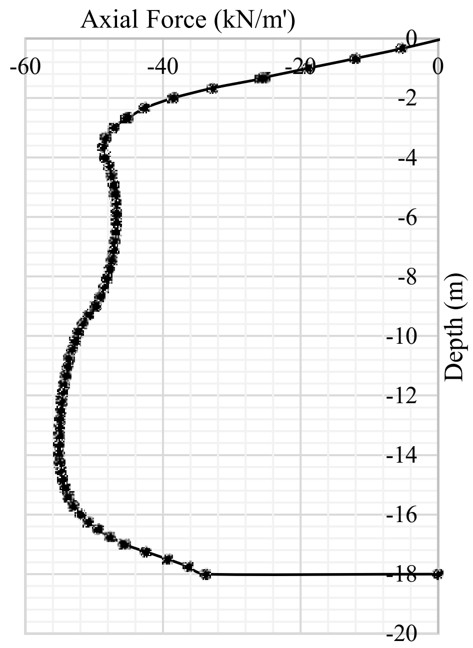

Fig. 11. The largest axial of pile for variations in pile depth of 18 m

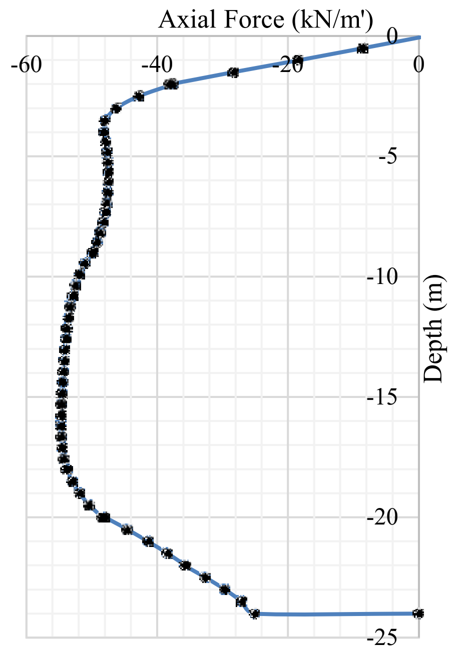

Fig. 13. The largest axial of pile for variations in pile depth of 24 m

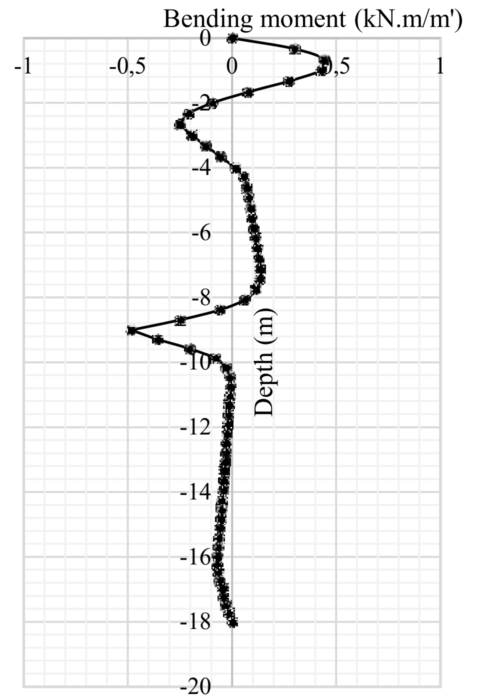

Fig. 12. The largest bending moment of pile for variations in pile depth of 18 m

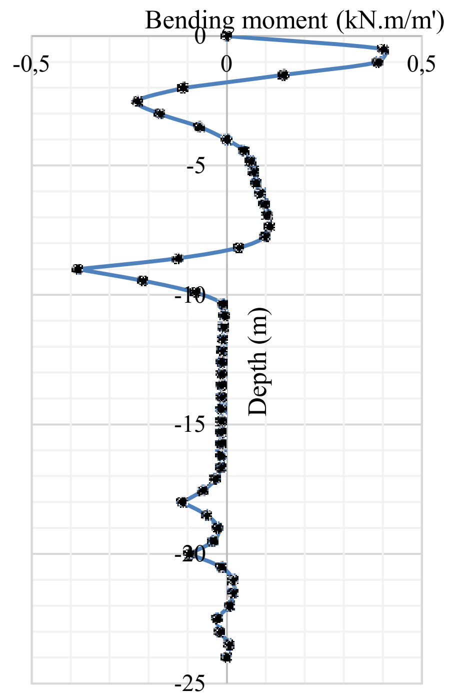

Fig. 14. The largest bending moment of pile for variations in pile depth of 24 m

Table 7. Recapitulation of output from PLAXIS

Depth of pile (m) (1)	Settlement (m) (2)	Bending moment (kN.m/m') (3)	Bending moment (kN.m) (4)	Axial force (kN/m') (5)	Axial force (kN) (6)
12	0.010	0.718	1.076	48.678	73.017
18	0.006	0.485	0.728	55.09	82.635
24	0.005	0.429	0.643	54.71	82.065

Table 7 shows 2 (two) bending moment columns but with different unit values. The bending moment value with units of kN.m (column 4) is obtained from the bending moment value with units of kN.m/m' (column 3) multiplied by the pile distance or spacing, which is 1.5m—the same for axial forces. In addition, the largest bending moment occurs on the pile at the edge, while the largest axial force appears on the pile in the middle. In Fig. 9 to 14, it can also be seen that there is a negative bending moment due to subgrade deformation.

From the analysis results, it was found that the settlement value will be smaller when the pile gets deeper (Fig. 15). For a pile length of 12 m, it has a settlement value of 0.01 m and decreases to 0.005 m for a pile length of 24 m—reduced settlement rate to 50% when the pile length is doubled. The depth of the piles used can be adjusted to the settlement conditions.

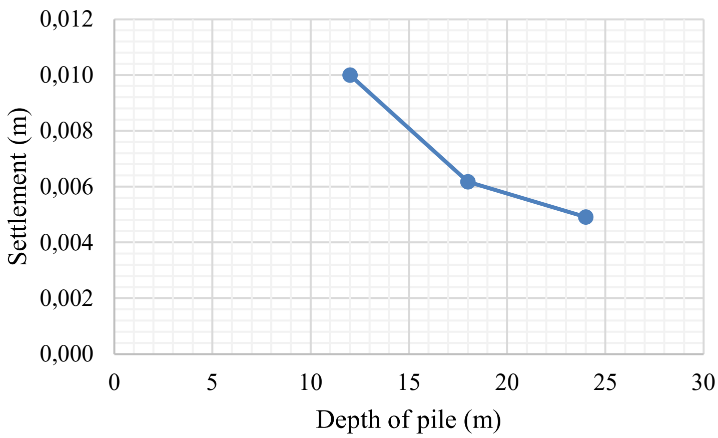

Fig. 15. Settlement value for variations in pile length

4. Conclusions

From the study results, it can be concluded that an analysis of subgrade reinforcement has been carried out using 3 (three) variations of pile depth. The modeling results in PLAXIS 2D revealed that settlement was obtained for each pile depth variation. Settlement will decrease if the pile depth is increased. The biggest settlement occurs in a pile that has a depth of 12 m. From the modeling results in PLAXIS 2D, the internal forces in the form of axial forces and moments that occur in each pile depth variation are obtained. The largest axial force occurs in the pile, which is in the middle of the embankment, while the greatest bending moment occurs in a pile at the edge of the embankment.

References

[1] Bowles, J.E. (1979). *Physical and geotechnical properties of soils*. New York, NY United States 10036.

[2] Tjie-Liong, G., Irsyam, M., and Gunawan, A. (2013). The Application Of Ground Improvement Techniques In Indonesia. In *18th Southeast Asian Geotechnical Conference (18SEAGC) & Inaugural AGSSEA Conference (1AGSSEA)*, 63–80. https:/www.doi.org/10.3850/978-981-07-4948-4_356.

[3] Kurniawan, J., Dite, A., Narendra, R., Evelyn, Widjaja, B., and Rahardjo, P. (2015). *Mitigation and Risk Reduction Of Mud Eruption Disaster In East Java Using Vacuum Consolidation Method*.

[4] Gouw, T.L., and Gunawan, A. (2020). Vacuum preloading, an alternative soft ground improvement technique for a sustainable development. *IOP Conf. Ser. Earth Environ. Sci.*, *426*,(1). https:/www.doi.org/10.1088/1755-1315/426/1/012003.

[5] Pratiwi, D.S. (2020). Evaluation of Soil Improvement Using Rapid Impact Compaction on Potentially Liquefiable Soil. *J. Rekayasa Hijau*, *4*(2), 82–92. https:/www.doi.org/10.26760/jrh.v4i2.82-92.

[6] Sams, M., He, W., Gamaliel, J., Mueller, M., and Kok, B. (2018). Design of Rapid Impact Compaction at the New Yogyakarta International Airport. *Intercational Conference on Geotechnics* (pp 39-48). IC Geotechnics.

[7] Gouw, T.L. (2018). Geosynthetics application in Indonesia - A case histories," *Geotech. Eng.*, *49*,(4), 132–144.

[8] Susila, E. and Agrensa, F. (2015). Case study on soft soil improvement using innovative and cost-effective reinforcing techniques. *J. Eng. Technol. Sci.*, *47*(2), 207–217. https:/www.doi.org/10.5614/j.eng.technol.sci.2015.47.2.10.

[9] Han, J., & Ye, S. L. (1991). Analysis of characteristics to composite grounds. In *Proceedings of First Young Asian Geotechnical Engineers Conference, Thailand* (pp. 197-206).

[10] Rahardjo, P.P., and Sugianto, A. (2018). The Use of Piled Plate to Support airport runway Embankment on Very Soft Soils Foundation..

[11] Fox, I., Du, M., and Buttling, S. (2004). Deep foundations for new international airport passenger terminal complex in Bangkok.

[12] Bowles, J.E. (1983). *Analysis and Design of Foundations Volume II*. Jakarta: Erlangga. (in Indonesia)

[13] Das, B.M., and Sivakugan, N. (2019). *Principles of Foundation Engineering, 9th Edition, SI Edition*.

[14] Bowles, J.E. (1997). *Foundation Analysis and Design International Fifth Edition*.